Propagation Characteristics of Microstrip Transmission Line on An Anisotropic Material Ridge

George W. Hanson, *Member, IEEE*

Abstract—**A microstrip transmission line residing on an electrically anisotropic material ridge embedded in a multilayered environment is studied using a coupled set of integral equations (IE's). The full-wave IE formulation easily accommodates arbitrary material anisotropy and inhomogeneity in the finite ridge region using equivalent polarization currents residing in a multilayered isotropic background. New results are presented for uniaxially anisotropic ridge structures which show that the transmission line propagation constant is sensitive to anisotropy for certain ridge structures and insensitive for others, compared to the conventional line on an infinite substrate. Results are also presented for a transmission line printed on a nonreciprocal solid-state magnetoplasma ridge. The current distribution associated with the dominant microstrip mode is investigated, where it is found that the transverse component of current is much larger for the ridge geometry than for the infinite substrate case, although the transverse component is still small compared to the longitudinal component.**

I. Introduction

CONVENTIONAL printed transmission lines employ continuous substrates in either an open or shielded environment. These structures have been previously studied, and the effect that substrate permittivity and anisotropy has on propagation characteristics has been determined for a wide range of practical configurations.

Recently, microstrip transmission lines on finite dielectric ridges have been investigated [1]–[8] as more complex circuit structures have become feasible. It has been shown that the ridge structure has several advantages compared to the traditional configuration of a transmission line over a wide substrate. For example, closely spaced lines on finite ridges decouple much faster with increasing separation, compared to the traditional configuration [1]. It is also found here that some microstrip ridge structures show other desirable characteristics, such as insensitivity to the presence of material anisotropy.

For microstrip ridge structures in a shielded environment, several different methods have been used to generate full-wave results. In [1], a combined integral equation/modal matching (IEMM) method is described. A method of lines (MOL) analysis is presented in [2], and a mixed potential mode-matching method is described in [3]. For open structures, a quasistatic method is presented in [4]. A mode-matching analysis of a microslab structure is presented in [5]. The MOL with absorbing boundary conditions (MOL/ABC) [6], and with a coordinate transformation (MOL/CT) [7], were used to provide full-wave results for the open ridge structure. An IE formulation is presented in [8], using an orthogonal wavelet expansion.

All of the previous analyses have assumed isotropic media. To fully investigate the properties of transmission lines on material ridges, the effect of anisotropy needs to be quantified, since many novel circuits utilize electrically anisotropic dielectrics. Also, many materials have some degree of natural anisotropy, or unintended anisotropy may be present due to material processing. This paper describes a theoretical formulation and numerical solution of a set of coupled integral equations which model the anisotropic ridge structure. The IE formulation was chosen since incorporation of anisotropy in the finite ridge region can be accounted for in a simple manner using equivalent polarization currents residing in a multilayered background. It is shown that anisotropy plays an important role for some ridge structures, while for other ridge geometries the dominant microstrip mode is insensitive to the presence of anisotropy.

Manuscript received February 1, 1995; revised August 1, 1995.

The author is with the Department of Electrical Engineering and Computer Science, University of Wisconsin-Milwaukee, Milwaukee, WI 53211 USA.

IEEE Log Number 9414850.

II. Theory

The geometry of interest is shown in Fig. 1(a). A perfectly conducting, infinitely thin microstrip transmission line and an anisotropic material waveguiding region reside in the cover region of a layered media background environment. A general permittivity dyadic given by

$$\overleftrightarrow{\epsilon}(x,z) = \begin{bmatrix} \epsilon_{xx} & \epsilon_{xy} & \epsilon_{xz} \\ \epsilon_{yx} & \epsilon_{yy} & \epsilon_{yz} \\ \epsilon_{zx} & \epsilon_{zy} & \epsilon_{zz} \end{bmatrix}$$

represents the anisotropic waveguiding region. A coupled set of IE's can be formed by enforcing boundary conditions along the surface of the transmission line and by forcing the total electric field in the waveguiding region to equal the sum of the impressed field and the field due to all currents in the system. These conditions can be expressed as

$$\hat{t} \cdot \{\vec{e}_x^{\,s}(x,d) + \vec{e}_{wg}^{\,s}(x,d)\} = -\hat{t} \cdot \vec{e}^{\,\mathrm{inc}}(x,d) \quad \cdots \forall x \in L \tag{1a}$$

$$\vec{e}(x,z) - \vec{e}_t^{\,s}(x,z) - \vec{e}_{wg}^{\,s}(x,z) = \vec{e}^{\,\mathrm{inc}}(x,z) \quad \cdots \forall (x,z) \in S_{wg} \tag{1b}$$

where L extends over the width of the microstrip line, S_{wg} denotes the space occupied by the anisotropic waveguiding region, $\hat{t}$ is a unit tangent vector to the transmission line, $\vec{e}_t^{\,s}$ is the scattered electric field maintained by conduction current on the transmission line, $\vec{e}_{wg}^{\,s}$ is the scattered electric field due

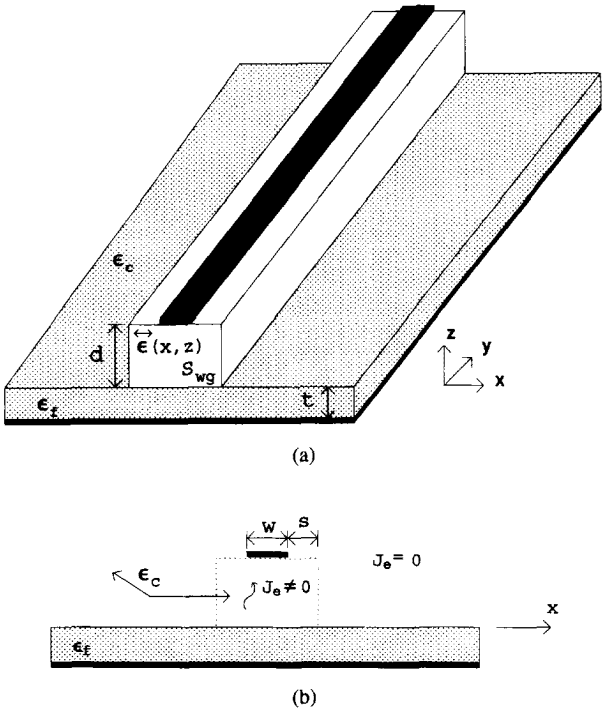

Fig. 1. (a) Anisotropic microstrip ridge structure; invariant along the y-axis. (b) Cross-sectional view of equivalent ridge structure obtained by replacing the anisotropic ridge media in (a) with isotropic media containing unknown currents.

to equivalent polarization current in the waveguide region, and $\vec{e}$ is the total electric field in the waveguide region. The field $\vec{e}^{\,\text{inc}}$ is an impressed field maintained by remote sources with the transmission line and waveguiding region absent but in the presence of the layered background. In the above, (1a) represents two scalar equations ($\hat{t} = \hat{x}, \hat{y}$ where $\hat{x}, \hat{y}$ are unit vectors in the x and y directions, respectively) which force the total tangential electric field to be zero along the perfectly conducting transmission line. Equation (1b) represents three scaler equations which force the total electric field at every point within the waveguiding region to equal the incident field plus the field maintained by the various currents. The radiation condition is enforced, along with boundary conditions at the other planar interfaces, by the Green's function for the background environment. An $e^{j\omega t}$ dependence is assumed and suppressed throughout.

Since the structure of interest is invariant along the y-axis, the following formulation is carried out in the one-dimensional spatial Fourier transform domain, with the transform pair $y \leftrightarrow k_y$. The electric field in the cover region is related to currents in the cover region by [9]

$$\vec{e}(\vec{\rho}, k_y) = \int_S \overleftrightarrow{G}^e(\vec{\rho} \mid \vec{\rho}', k_y) \cdot \vec{J}(\vec{\rho}', k_y) dS' \tag{2}$$

where $\overleftrightarrow{G}^e$ is an electric dyadic Green's function for the multilayered background environment with the waveguiding region and transmission line absent, provided in the Appendix for convenience.

The inhomogeneous anisotropic waveguide/cover region is replaced by a homogeneous isotropic cover region containing equivalent polarization currents which reside in the space previously occupied by the waveguide and vanish outside of that region, as shown in Fig. 1(b). The equivalent currents can easily be derived from Maxwell's equations to yield

$$\vec{J}_e(x,z) = j\omega[\overleftrightarrow{\epsilon}(x,z) - \epsilon_c \overleftrightarrow{I}] \cdot \vec{e}(x,z). \tag{3}$$

A coupled set of IE's is formed by substituting the various electric field contributions from polarization and conduction currents into (1), yielding

$$\begin{aligned} \hat{t} \cdot \Bigg\{ & \int_x \overleftrightarrow{G}^e(x, d \mid x', d) \cdot \vec{J}_c(x') dx' \\ & + j\omega \int_{S_{wg}} \overleftrightarrow{G}^e_a(x, d \mid x', z') \cdot \vec{e}(x', z') dS' \Bigg\} \\ & = -\hat{t} \cdot \vec{e}^{\,\text{inc}}(x, d) \end{aligned} \tag{4}$$

for $\hat{t} = \hat{x}, \hat{y}; -\frac{w}{2} < x < \frac{w}{2}$ from (1a), and

$$\begin{aligned} & \vec{e}(x,z) - \int_x \overleftrightarrow{G}^e(x, z \mid x', d) \cdot \vec{J}_c(x') dx' \\ & - j\omega \int_{S_{wg}} \overleftrightarrow{G}^e_a(x, z \mid x', z) \cdot \vec{e}(x', z') dS' \\ & = \vec{e}^{\,\text{inc}}(x, z) \end{aligned} \tag{5}$$

for all $x, z \in S_{wg}$ from (1b). The notation $\overleftrightarrow{G}^e_a = \overleftrightarrow{G}^e \cdot [\overleftrightarrow{\epsilon} - \epsilon_c \overleftrightarrow{I}]$ is introduced for convenience.

The coupled set of IE's is solved using the method of moments (MoM). The conduction currents on the transmission line are expanded as

$$\vec{J}_c(x) = \hat{x} \sum_{n=0}^{N_x} a_n^x f_n^x(x) + \hat{y} \sum_{n=0}^{N_y} a_n^y f_n^y(x) \tag{6}$$

where the a's are unknown expansion constants and the f_n^α are known functions chosen to model the expected current. Edge-weighted Chebyshev polynomials were chosen here since they have shown good convergence for coupled transmission lines residing on infinite substrates [10]. The functions are explicitly given as

$$\begin{aligned} f_n^x(x) &= \sqrt{1 - \left(\frac{x}{w}\right)^2}\, U_n\left(\frac{x}{w}\right), \\ f_n^y(x) &= \frac{1}{\sqrt{1 - \left(\frac{x}{w}\right)^2}} T_n\left(\frac{x}{w}\right) \end{aligned} \tag{7}$$

where T_n, U_n are Chebyshev polynomials of the first and second kinds, respectively.

The electric field in the waveguide region is expanded using subdomain basis functions

$$\vec{e}(x,z) = \sum_{\beta=x,y,z} \sum_{n=1}^{N} \sum_{m=1}^{M} \hat{\beta} e^{\beta}_{n,m} P_n(x) R_m(z) \tag{8}$$

where

$$P_n(x) = \begin{cases} \frac{\sin[k_e(h - |x - x_n|)]}{\sin(k_e h)} & |x - x_n| < h \\ 0 & \text{else} \end{cases}$$

are overlapping piecewise sinusoidal (PWS) functions, with $R_m(z)$ having a similar definition. In order to allow for non-vanishing fields along the perimeter of the waveguide region,

half-PWS functions are used at $x = -(w/2+s), (w/2+s)$ and $z = 0, d$. These subdomain functions were chosen because they are numerically well-behaved functions which reduce to triangular functions for small values of k_e. It was found that fastest convergence was obtained by setting the wavenumber to be $k_e \approx 0.01k_0 - 0.1k_0$, thereby effectively utilizing triangular functions. Two-dimensional pulse functions were also tried but they did not yield values of the propagation constant which converged as a function of the number of pulses, probably due to their discontinuous nature.

A galerkin solution is implemented by testing each scaler IE with the appropriate function, leading to a matrix system $[Z(k_y)]\begin{bmatrix} a \\ b \end{bmatrix} = [b]$, where the RHS comes from an external excitation. To determine propagation constants (k_y), the RHS is set to zero and a numerical root search is performed to find the value of k_y which forces the determinate of the impedance matrix to vanish. The nullspace of the impedance matrix yields the modal currents associated with each propagation mode.

III. Results

For the following results concerning a microstrip transmission line residing on a material ridge over an infinite ground plane, the dominant microstrip mode is investigated. All permittivities are relative to ϵ_0, and $\mu = \mu_0$. A detailed convergence study was performed but is not presented here. Generally though, convergence was very rapid with respect to the number of Chebyshev polynomials for the microstrip current (both longitudinal and transverse components), where 3–5 functions were found to be sufficient. Similarly, 5–7 PWS modes yielded accurate results for the waveguide field in the direction normal to the ground plane (z). The required number of PWS modes in the transverse direction (x) was strongly dependent on the ratio s/w. For $s/w = 0$, 3–5 modes were sufficient, while for $s/w = 0.5$, 30–40 modes were necessary to obtain good convergence. This is due to the rapid field variation for line $|x| > (w/2 + s)$ in the vicinity of the microstrip.

Extensive numerical tests were conducted to verify the method presented here. The top two sets of dispersion curves in Fig. 2 compare results obtained using this method with MOL full-wave results from [6], [7], [11] for a microstrip transmission line on an isotropic dielectric ridge ($\epsilon = 9.7$) over an infinite ground plane ($t = 0$). The effective refractive index versus frequency is shown for the cases $s/w = 0$ and $s/w = 0.5$. Results of the IE method described here agree very well with the MOL/ABC method [6], [11]. The bottom dispersion curve compares results obtained using this method with results from [12] for a strip dielectric waveguide (Fig. 1 with conducting transmission line removed). Results using this method are seen to agree very well with previously published results. Although not shown here, this method also reproduced the results of [13] for a microstrip transmission line over an infinite substrate (Fig. 1 with ridge removed), and for anisotropic dielectric waveguides considered in [12], [14], among others.

Fig. 3 shows some effects of anisotropy on the microstrip ridge structure. Results are shown for a transmission line on an infinite substrate [15], and for the ridge structure with $s/w = 0, 0.25, 0.5$. The waveguiding material is assumed to be uniaxially anisotropic, characterized by

$$\overleftrightarrow{\epsilon} = R(\theta,\phi)\begin{bmatrix} \epsilon_\perp & 0 & 0 \\ 0 & \epsilon_\perp & 0 \\ 0 & 0 & \epsilon_\parallel \end{bmatrix} R^T(\theta,\phi)$$

where the $R(\theta,\phi)$ is an orthogonal rotation matrix which rotates the optic axis of the material about the fixed xyz coordinate system [16], (θ,ϕ) represent the usual spherical angles and $R(0,0) = [I]$, the identity matrix. The permittivity components $\epsilon_\perp, \epsilon_\parallel$ represent the component of permittivity perpendicular and parallel to the optic axis, respectively. Results are shown for an isotropic dielectric ($\epsilon_\perp = \epsilon_\parallel = 11.6$) and an anisotropic dielectric ($\epsilon_\perp = 9.4$, $\epsilon_\parallel = 11.6$) with $\theta = \phi = 0$. It can be seen that for the infinite substrate case ($s/w = \infty$) the presence of anisotropy significantly affects the propagation constant of the structure. For the ridge with $s/w = 0$, the electric field under the microstrip line is primarily vertically directed, with the fringing field in the isotropic cover region, and so the propagation constant is governed by the z-component ($\epsilon_\parallel$) of permittivity. For this case the isotropic and anisotropic curves overlay each other. The $s/w = 0.25$ case is also very insensitive to the presence of anisotropy, while the $s/w = 0.5$ case displays similar characteristics to the $s/w = \infty$ case.

The sensitivity to anisotropy is again investigated in Fig. 4, which shows the propagation constant versus the components of permittivity tangential to the surface ($\epsilon_\perp$), with $\epsilon_\parallel = 11.6$ and $\theta = \phi = 0$. In this figure, the infinite substrate case is shown along with $s/w = 0, 0.25, 0.5$ at 30 GHz. It is seen that tangential components of permittivity don't affect the $s/w = 0$ ridge structure, and only slightly influence the $s/w = 0.25$ structure at this frequency.

Fig. 5 shows dispersion curves for the microstrip ridge structure for the special case $s/w = 0$ for several different orientations of the optic axis with $\epsilon_\perp = 5.12$, $\epsilon_\parallel = 3.4$. Rotation by $\theta \neq 0$ (in the plane containing the z-axis) introduces $\epsilon_{xz} = \epsilon_{zx}$ permittivity elements, while rotation by $\theta, \phi \neq 0$ result in all off-diagonal components of permittivity being nonzero. It is seen that for more complicated forms

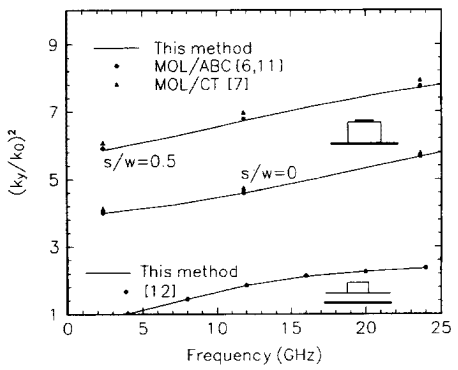

Fig. 2. Comparison of results obtained using this method and other analyses. Top two sets of curves: Microstrip ridge structure with $s/w = 0$ and $s/w = 0.5, w = d = 0.127$ cm, $\epsilon = 9.7, t = 0$.Bottom curve: strip dielectric waveguide with $\epsilon_f = 2.62, \epsilon = 2.55, t = 0.5$ cm, $d = 0.32$ cm, $(w + 2s) = 0.65$ cm.

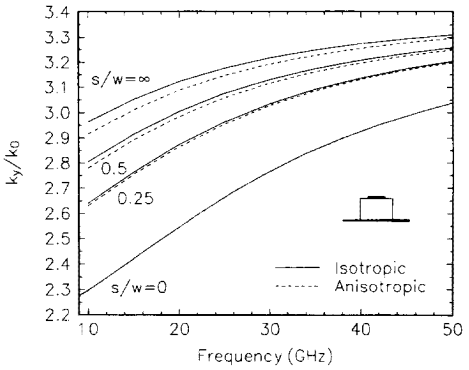

Fig. 3. Dispersion curve for isotropic and anisotropic microstrip ridge structures with $s/w = \infty$ [15] and $s/w = 0, 0.25, 0.5$, and $w = d = 0.127$ cm, $t = 0$. Isotropic case: $\epsilon_\perp = \epsilon_{||} = 11.6$, isotropic case: $\epsilon_\perp = 9.4$, $\epsilon_{||} = 11.6$.

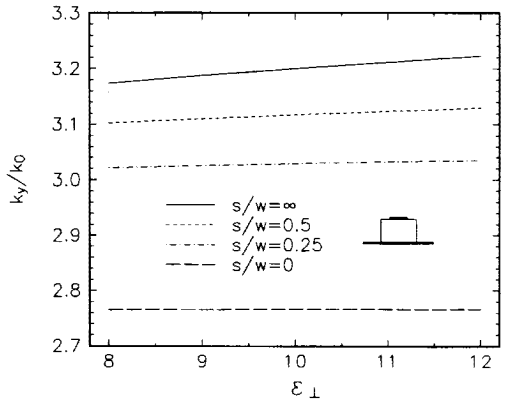

Fig. 4. Normalized propagation constant versus tangential components of permittivity for several microstrip ridge geometries. Frequency = 30 GHz, $w = d = 0.127$ cm, $\epsilon_{||} = 11.6, t = 0$.

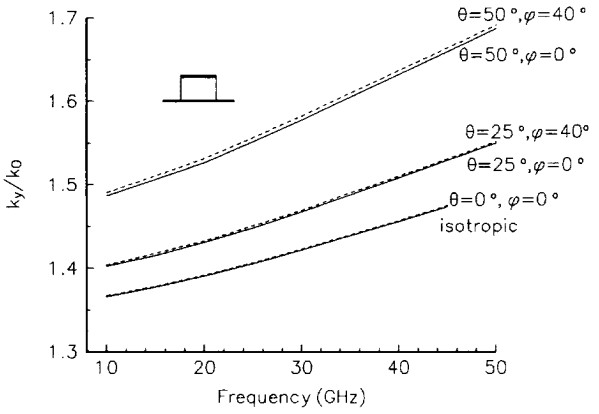

Fig. 5. Dispersion curve for isotropic and anisotropic microstrip ridge structure for $s/w = 0, w = d = 0.1$ cm, $t = 0$. Angle of optic axis varies. $\epsilon_\perp = 5.12$, $\epsilon_{||} = 3.4$. Isotropic case: $\epsilon = \epsilon_{||}$

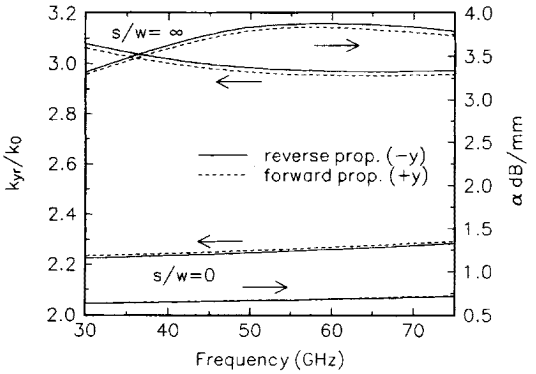

Fig. 6. Dispersion curve for nonreciprocal propagation on a magnetoplasma ridge structure, with the magnetic bias field in the x-direction, $w = d = .01$ cm, $\epsilon_s = 12.5$, $\tau_p = 1$ ps, $n = 10^{14}$ cm^{-3}, $B_0 = 15$ kG.

of anisotropy, the $s/w = 0$ case is somewhat sensitive to anisotropy, since, for example, while varying ϕ the vertical component of permittivity does not change but the propagation constant does change slightly.

Fig. 6 shows the forward and reverse propagation constant for a transmission line printed on a solid-state magnetoplasma material. This material can be formed by applying a dc magnetic bias field to a semiconductor, and transmission lines utilizing the resulting nonreciprocal propagation have been described in many papers (e.g., [17], [18]). When the magnetic bias field is applied along the x-direction, the permittivity dyad is given by

$$\overleftrightarrow{\epsilon} = \begin{bmatrix} \zeta & 0 & 0 \\ 0 & \xi & -j\eta \\ 0 & j\eta & \xi \end{bmatrix}$$

with

$$\zeta = +\epsilon_s \frac{\omega_p^2}{j\omega\left(j\omega + \frac{1}{\tau_p}\right)}, \quad \xi = \epsilon_s + \frac{\omega_p^2\left(j\omega + \frac{1}{\tau_p}\right)}{j\omega\left[\omega_c^2 + \left(j\omega + \frac{1}{\tau_p}\right)^2\right]},$$

$$\eta = \frac{\omega_p^2 \omega_c}{\omega\left[\omega_c^2 + \left(j\omega + \frac{1}{\tau_p}\right)^2\right]}$$

where $\omega_p^2 = ne^2/\epsilon_0 m^*$ is the plasma frequency, $\omega_c = |e|B_0/m^*$ is the cyclotron frequency, n is the carrier concentration, e is the electron charge, m^* is the effective mass, B_0 is the applied dc magnetizing field, τ_p is the momentum relaxation time, and ϵ_s is the relative permittivity of the material. The material is assumed to be GaAs ($m^* = 0.067m_e$ where m_e is the rest mass), with $\epsilon_s = 12.5$, $\tau_p = 1$ ps, $n = 10^{14}$ cm^{-3}, $B_0 = 15$ kG. Open microstrip lines deposited over this type of substrate were analyzed in [18]. The method described in [15] was used to reproduce those results for $s/w = \infty$, which are shown along with the $s/w = 0$ case in Fig. 6. It can be seen that the $s/w = 0$ case retains the nonreciprocal behavior, but the differential phase shift between the forward and reverse phase constants ($\mathrm{Re}\{k_y\} = k_{yr}$) is slightly diminished. This is again explained by the fact that the line is primarily affected by the vertical component of permittivity since the fringing fields exist only in the air region. Attenuation α (proportional to $\mathrm{Im}\{k_y\}$) is also significantly reduced since the imaginary part of the vertical component of permittivity is relatively small compared to the imaginary part of the other permittivity components.

Fig. 7 shows the transverse and longitudinal components of modal current on the transmission line associated with the dominant microstrip mode, normalized by the longitudinal

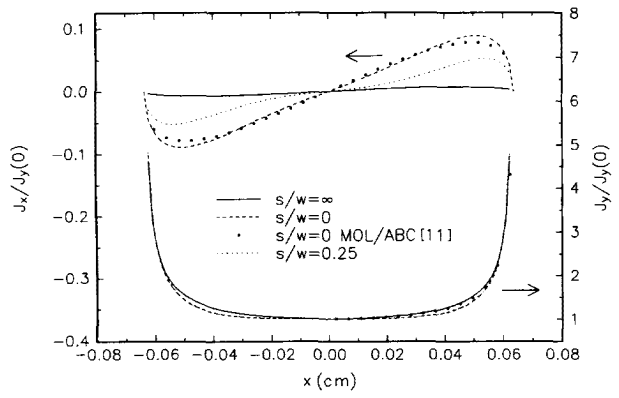

Fig. 7. Modal current versus position along the microstrip. Frequency = 11.811 GHz ($d/\lambda_0 = 0.05$), $w = d = 0.127$ cm, $\epsilon_\perp = \epsilon_\parallel = 9.7, t = 0$.

current evaluated at the center of the conductor. It is believed that the model current distribution of microstrip lines on ridges has not been described in the literature as yet. Results are shown for $s/w = 0, 0.25$, and for the infinite substrate case obtained from [15], along with results from [11] for the $s/w = 0$ case. Current distributions for isotropic ridges ($\epsilon = 9.7$) are shown since it was found the presence of anisotropy had only a slight effect on the current distribution for these cases. The longitudinal component is shown to be insensitive to the s/w ratio. It can be observed that the transverse current on the ridge structure is much larger than for the conventional geometry, although it is still small compared to the longitudinal component. This would indicate that this component of current, which is often ignored in MoM analyses especially at low frequencies, may play a more important role for microstrip ridge structures. The effect on the propagation constant of ignoring the transverse component of current has not been studied here.

IV. Conclusion

Microstrip transmission lines residing on electrically anisotropic material ridges have been studied using a coupled set of integral equations. The IE formulation accommodates the incorporation of anisotropy in the finite ridge region using equivalent volume polarization currents. Results are presented which show that the transmission line propagation constant is relatively insensitive to the presence of anisotropy for certain ridge structures, compared to the conventional line on an infinite substrate. The modal microstrip transmission line current has been studied, where it was found that the transverse component of current is much larger for the ridge structure than for the conventional microstrip geometry.

Appendix

The electric dyadic Green's function is given by [9]

$$\overleftrightarrow{G}^e(\vec{\rho} \mid \vec{\rho}', k_y) = P.V.\ (k_c^2 + \nabla\nabla\cdot)\overleftrightarrow{G}_\pi(\vec{\rho}' \mid \vec{\rho}', k_y) + \overleftrightarrow{L}\delta(\vec{\rho} - \vec{\rho}') \tag{A1}$$

where the depolarizing dyad term is $\overleftrightarrow{L} = -\hat{z}\hat{z}/j\omega\epsilon_c$. The Green's function $\overleftrightarrow{G}_\pi$ is a Hertzian potential Green's dyadic given as

$$\overleftrightarrow{G}_\pi(\vec{\rho} \mid \vec{\rho}') = \overleftrightarrow{I}\, G^p + (\hat{x}\hat{x} + \hat{y}\hat{y})G_t^r + \hat{z}\left[\frac{\partial G_c^r}{\partial x}\hat{x} + G_n^r\hat{z} + \frac{\partial G_c^r}{\partial y}\hat{y}\right] \tag{A2}$$

where

$$G^p(\vec{\rho} \mid \vec{\rho}') = \frac{\eta_c}{jk_c}\int_{-\infty}^{\infty} \frac{e^{jk_x(x-x')}e^{-p_c|z-z'|}}{2(2\pi)p_c}dk_x \tag{A3}$$

is the principal potential and

$$\begin{Bmatrix} G_t^r(\vec{\rho} \mid \vec{\rho}') \\ G_n^r(\vec{\rho} \mid \vec{\rho}') \\ G_c^r(\vec{\rho} \mid \vec{\rho}') \end{Bmatrix} = \frac{\eta_c}{jk_c}\int_{-\infty}^{\infty} \begin{Bmatrix} R_t(k_x, k_y) \\ R_n(k_x, k_y) \\ C(k_x, k_y) \end{Bmatrix} \times \frac{e^{jk_x(x-x')}e^{-p_c(z-z')}}{2(2\pi)p_c}dk_x \tag{A4}$$

yields the reflected potential. Coefficients are given as

$$R_t = \frac{N_1}{Z^h}, \quad R_n = \frac{N_2}{Z^e}, \quad C = \frac{2(N_{fc}^2 - 1)p_c}{Z^h Z^e}$$

where

$$\begin{aligned} N_1 &= p_c - p_f \coth(p_f t) \\ N_2 &= N_{fc}^2 p_c - p_f \tanh(p_f t) \\ Z^e &= N_{fc}^2 p_c + p_f \tanh(p_f t) \\ Z^h &= p_c + p_f \coth(p_f t) \end{aligned}$$

and $N_{fc}^2 = \epsilon_f/\epsilon_c, p_{f,c} = \sqrt{k_x^2 + k_y - k_{f,c}^2}$, $\eta_c = \sqrt{\mu_c/\epsilon_c}$, $k_{f,c} = \omega\sqrt{\mu_{f,c}\epsilon_{f,c}}$. For the case of a ridge on a ground plane ($t = 0$), $R_t = -1$, $R_n = 1$, $C = 0$.

The Green's function (A1) should be treated in the distributional sense; it must operate on a current to be meaningful. Subsequent to performing spatial integrals of (A3) and (A4), implicated by (4) and (5) and the Galerkin procedure, the spectral integrals over k_x are rendered convergent. The principal value (PV) nature of (A1) can be implemented by excluding the $z = z'$ point from the spatial integrals using a δ region. The final MoM matrix entries can be evaluated with $\lim_{\delta\to 0}$.

Acknowledgment

The author gratefully acknowledges Reinhold Pregla for providing his MOL/ABC results, and for helpful comments made by one of the reviewers.

References

[1] A. G. Engel and L. P. B. Katehi, "Frequency and time domain characterization of microstrip-ridge structures," *IEEE Trans. Microwave Theory Tech.*, vol. 41, pp. 1251–1261, Aug. 1993.

[2] M. Thorburn, A. Agoston, and V. K. Tripathi, "Computation of frequency-dependent propagation characteristics of microstriplike propagation structures with discontinuous layers," *IEEE Trans. Microwave Theory Tech.*, vol. 38, pp. 148–153, Feb. 1990.

[3] C. C. Tzuang and J. Tseng, "A full-wave mixed potential mode-matching method for the analysis of planar or quasiplanar transmission lines," *IEEE Trans. Microwave Theory Tech.*, vol. 39, pp. 1701–1711, Oct. 1991.

[4] C. E. Smith and R. S. Chang, "Microstrip transmission line with finite-width dielectric," *IEEE Trans. Microwave Theory Tech.*, vol. MTT-28, pp. 90–94, Feb. 1980.
[5] B. Young and T. Itoh, "Analysis and design of Microslab waveguide," *IEEE Trans. Microwave Theory Tech.*, vol. MTT-35, pp. 850–857, Sept. 1987.
[6] A. Dreher and R. Pregla, "Analysis of microstrip structures with an inhomogeneous dielectric layer in an unbounded region," *IEE Electron. Lett.*, vol. 28, pp. 2133–2134, 1992.
[7] X. H. Yang and L. Shafai, "Full wave approach for the analysis of open planar waveguides with finite width dielectric layers and ground planes," *IEEE Trans. Microwave Theory Tech.*, vol. 42, pp. 142–149, Jan. 1994.
[8] K. Sabetfakhri and L. P. B. Katehi, "Analysis of integrated millimeter-wave and submillimeter-wave waveguides using orthonormal wavelet expansions," *IEEE Trans. Microwave Theory Tech.*, vol. 42, pp. 2412–2422, Dec. 1994.
[9] J. S. Bagby and D. P. Nyquist, "Dyadic Green's functions for integrated electronic and optical circuits," *IEEE Trans. Microwave Theory Tech.*, vol. MTT-35, pp. 206–210, Feb. 1987.
[10] J. S. Bagby, C. Lee, Y. Yuan, and D. P. Nyquist, "Entire-domain basis MoM analysis of coupled microstrip transmission lines," *IEEE Trans. Microwave Theory Tech.*, vol. 40, pp. 49–57, Jan. 1992.
[11] R. Pregla, Private communication, *Electromagnetics* paper forthcoming.
[12] F. Olyslager and D. De Zutter, "Rigorous boundary integral equation solution for general isotropic and uniaxial anisotropic dielectric waveguides in multilayered media including losses, gain and leakage," *IEEE Trans. Microwave Theory Tech.*, vol. 41, pp. 1385–1392, Aug. 1993.
[13] M. Kobayashi and F. Ando, "Dispersion characteristics of open microstrip lines," *IEEE Trans. Microwave Theory Tech.*, vol. MTT-35, pp. 101–105, Feb. 1987.
[14] M. Koshiba, K. Hayata, and M. Suzuki, "Approximate scalar finite-element analysis of anisotropic optical waveguides with off-diagonal elements in a permittivity tensor," *IEEE Trans. Microwave Theory Tech.*, vol. MTT-32, pp. 587–593, June 1984.
[15] G. W. Hanson, "Integral equation formulation for inhomogeneous anisotropic media Green's dyad with application to microstrip transmission line propagation and leakage," *IEEE Trans. Microwave Theory Tech.*, vol. 43, pp. 1359–1363, June 1995.
[16] J. A. Kong, *Electromagnetic Wave Theory*, 2nd Ed. New York: Wiley, 1990.
[17] C. M. Krowne, A. A. Mostafa, and K. A. Zaki, "Slot and microstrip guiding structures using magnetoplasmons for nonreciprocal millimeter-wave propagation," *IEEE Trans. Microwave Theory Tech.*, vol. 36, pp. 1850–1860, Dec. 1988.
[18] F. Mesa and M. Horno, "Application of the spectral domain method for the study of surface slow waves in nonreciprocal planar structures with a multilayered gyroelectric substrate," *IEEE Proc-H.*, vol. 140, pp. 193-200, June 1993.

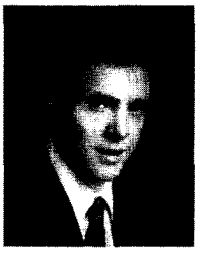

George W. Hanson (S'89–M'91) was born in Glen Ridge, NJ, in 1963. He received the B.S.E.E. degree from Lehigh University, Bethlehem, PA, the M.S.E.E. degree from Southern Methodist University, Dallas, TX, and the Ph.D. degree from Michigan State University, E. Lansing, in 1986, 1988, and 1991, respectively.

From 1986 to 1988, he was a Development Engineer with General Dynamics in Fort Worth, TX, where he worked on radar simulators. From 1988 to 1991 he was a Research and Teaching Assistant in the Department of Electrical Engineering at Michigan State University. He is currently Assistant Professor of Electrical Engineering at the University of Wisconsin in Milwaukee. His research interests include electromagnetic interactions in layered media, microstrip circuits, and microwave characterization of materials.

Dr. Hanson is a member of URSI Commission B, Sigma Xi, and Eta Kappa Nu.